Polymer Chemistry

Accepted Manuscript

ROYAL SOCIETY OF CHEMISTRY

www.rsc.org/polymers

Polymer Chemistry

RSCPublishing

ARTICLE

Light-Stimulated Mechanically Switchable, Photopatternable Cellulose Nanocomposites

Cite this: DOI: 10.1039/x0xx00000x

Mahesh V. Biyani, Mehdi Jorfi, Christoph Weder, and E. Johan Foster*

Received ooth April 2014,
Accepted ooth April 2014

DOI: 10.1039/x0xx00000x

www.rsc.org/

We report light-responsive, mechanically switchable, photopatternable nanocomposites based on benzophenone-derivatized cellulose nanocrystals (Bp-CNCs). Bp-CNCs are highly photoreactive and undergo radical-mediated reactions upon UV exposure, which were exploited to create materials with switchable mechanical characteristics. The nanocomposites were fabricated by incorporating 10 or 20% w/w Bp-CNCs into a rubbery ethylene oxide/epichlorohydrin copolymer (EO-EPI) matrix. The introduction of Bp-CNCs caused a pronounced stiffness increase. The tensile storage modulus (E') increased from 4 MPa (neat polymer) to 222 MPa and 407 MPa for nanocomposites with 10% w/w or 20% w/w Bp-CNCs. E' further increased to 293 MPa and 508 MPa upon irradiation with 365 nm UV light, on account of formation of covalent bonds between the Bp-CNCs and between the Bp-CNCs and the matrix polymer. The photoreaction reduced the level of aqueous swelling of the nanocomposites, as well as the extent of water-induced softening. The properties can be changed in a spatially-resolved manner and the new nanocomposites also exhibit shape memory properties.

Introduction

Polymer nanocomposites have emerged as fascinating materials, due to their remarkable strength, outstanding barrier properties, improved thermal and solvent stability and flame resistance.[1-6] The reinforcing elements within nanocomposites not only provide an opportunity to improve the strength and modulus of the material, but can also be utilized to impart the materials with stimuli-responsive characteristics (*vide infra*). In this context, highly crystalline, rod-shaped nanoparticles of cellulose (cellulose nanocrystals, CNCs) have emerged as useful nanofillers, which can be isolated from a broad range of natural sources *via* acid hydrolysis, enzymatic hydrolysis, or mechanical treatment.[7-26] The authors, as well as others, have shown in a series of previous contributions that the manipulation of the interactions between CNCs and between the CNCs and the polymer matrices can serve as basis for stimuli-responsive, mechanically adaptive materials that are possibly useful for biomedical and other applications.[27-34] Most of the reported mechanically adaptive nanocomposites are water-responsive; the formation of a hydrogen-bonded CNC network causes these materials to exhibit high stiffness when dry, but upon exposure the CNC network is disrupted and the materials soften. Several recent examples suggest that it is possible to make the responsiveness of such materials more specific to certain stimuli. Way *et al.* reported pH-responsive CNC-based nanocomposites that exploit the responsive nature of amine-decorated and carboxylated CNCs, *i.e.*, the possibility to moderate filler-filler interactions *via* their state of protonation.[35] We reported optically healable supramolecular nanocomposites, assembled from CNCs and telechelic poly(ethylene-*co*-butylene) bearing the quadruple hydrogen bonding ureidopyrimidone motif. These materials display an intriguing combination of high stiffness, high strength, and rapid and efficient optical healing, which appears to result from the specific design, *i.e.*, the full integration of filler and matrix and the ability to disassemble the hydrogen-bonding motifs *via* a light-heat conversion process.[36] In the same context, Fox *et al.* utilized light-activated thiol-ene click chemistry to create nanocomposites that mimic the graduated mechanical properties of squid beaks utilizing allyl functionalized CNCs.[37] In a recent study, we introduced light-responsive mechanically adaptive nanocomposites, in which light can be used to change the interactions between CNCs, and therewith the mechanical properties of the materials, under "closed-system conditions" and in a rather specific manner.[38] The nanocomposites were prepared by reinforcing a rubbery ethylene

oxide/epichlorohydrin copolymer (EO-EPI) matrix with coumarin-decorated CNCs. This design was based on the well-established fact that coumarin derivatives can undergo dimerization reactions upon exposure to ultraviolet (UV) light with a wavelength of >300 nm. While the as-prepared nanocomposites already show a significantly increased stiffness in comparison to the neat EO-EPI matrix, the stiffness increased further upon irradiation with UV light. While the properties of these materials are believed to change mainly on account of optically-induced changes of interactions among CNCs (*i.e.*, the formation of covalent bonds between the coumarin moieties through a 2+2 cycloaddition), we here report an alternative approach that exploits a less specific photoreactive motif. In this case, the predominant reaction to be expected - on the grounds of relative concentrations - is the formation of covalent bonds between CNCs and the matrix polymer. Thus, the chemistry exploited here is the UV light-activation of benzophenone (Bp), which leads to the formation of reactive excited states that preferentially consume nearby C-H bonds to form new C-C bond.[39, 40] Bp has been widely used for applications that range from photopatterning to the use as photoinitiator in polymerization and represents a well behaved, reliable photoactive moiety.[41-44] In addition, benzophenone has also been used to decorate cotton fabrics by Hong and co-workers for antimicrobial application and as a photoinitiator for graft polymerization.[45, 46] We hypothesized that benzophenone-derivatized CNCs (Bp-CNCs) would be an interesting basis for a new class of light-activated mechanically adaptive materials, in which light exposure can trigger the rapid formation of bonds among CNCs and (presumably preferentially) between CNCs and the surrounding polymer matrix (Scheme 1 and Fig. 1). Therefore, CNCs were decorated with a benzophenone derivative (Scheme 1) and the resulting Bp-CNCs were utilized for the preparation of nanocomposites with a rubbery EO-EPI matrix, which was chosen to permit comparison of the new materials with previously studied systems.[32, 47] The mechanical properties of these materials were examined as a function of composition, exposure to UV light, and exposure to water. Furthermore, we also explore the possibility of photopatterning and the light-activated shape fixing properties of the new EO-EPI/Bp-CNCs nanocomposites.

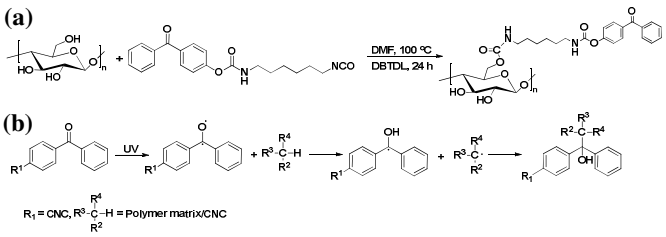

Scheme 1 (a) Derivatization of cellulose nanocrystals (CNCs) with 4-benzoylphenyl (6-isocyanatohexyl) carbamate (Bp-NCO). (b) Generalized reaction of the Bp-motif with an aliphatic residue (of another CNC or the polymer matrix) upon UV irradiation.

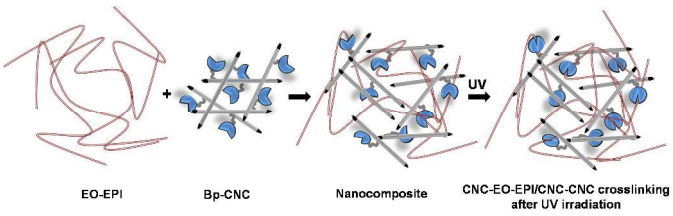

Fig. 1 Schematic representation of the process used to prepare EO-EPI/Bp-CNC nanocomposites and the architecture of these materials before (open jaw) and after UV exposure (closed jaw).

Experimental Section

Materials

4-Hydroxybenzophenone, hexamethylene diisocyanate (HMDI), dibutyltindilaurate (DBTDL), and hexane were purchased from Sigma Aldrich. N,N-Dimethylformamide (DMF) extra dry over molecular sieves was purchased from Acros Organics. The ethylene oxide/epichlorohydrin copolymer (EO-EPI) was obtained from Daiso Co. Ltd. Osaka, Japan (Epichlomer, co-monomer ratio = 1:1, density = 1.39 g/cm^3, Mw ca. 1 x 10^6 g mol^{-1}). All chemicals were used without further purification. CNCs were isolated by sulfuric acid hydrolysis from tunicates (Styela clava) following the previously published protocol.[36] The sulfate concentration on the surface of the CNCs, left over from the isolation process of CNCs from native material, was found to be 76.2 mmol/kg using standard conductometric titration protocols.[36] The aerogels of CNCs were obtained by lyophilizing liquid nitrogen frozen aqueous CNC dispersion produced after the hydrolysis using a VirTis BenchTop 2K XL lyophilizer. Please note: As HMDI and DBTDL are potentially harmful chemicals, they should be handled with appropriate laboratory procedures.

Analytical Methods

^{1}H-NMR (300 MHz, 200 scans) spectra were recorded in CDCl3 at room temperature on a Bruker Avance III 300 MHz. Chemical shifts are expressed in ppm relative to internal TMS standard. FT-IR spectra were collected in ATR mode between 4000-600 cm^{-1} using vacuum-dried samples on a Perkin Elmer Spectrum 65 spectrometer with a resolution of 4 cm^{-1} and 50 scans per sample. UV-visible absorbance spectroscopy was used to monitor the level of functionalization of the CNCs and the photoreactions of Bp-CNC. The spectra were acquired using DMF as a solvent for Bp-CNCs and Bp-NCO on a Shimadzu UV-2401 PC spectrophotometer in the wavelength range of 200-400 nm.

Transmission Electron Microscopy (TEM)

TEM images were acquired on Philips CM100 Bio-microscope operated at an accelerating voltage of 80 kV to study the dispersion as well as the morphology of unmodified and modified cellulose nanocrystals. Sample preparation involved depositing 2 µL of a dispersions of CNCs/Bp-CNC in DMF (CNC content = 0.1 mg/mL) onto carbon-coated grids (Electron

Microscopy Sciences) and drying the sample in an oven at 70 ºC for 4 h. The CNC and Bp-CNC dimensions were determined by analyzing 5 TEM images individually for both type of CNCs and measuring length and width of more than 100 CNCs using image tool software. The dimensions thus determined are reported as average values ± standard error.

Synthesis of 4-benzoylphenyl (6-isocyanatohexyl) carbamate (Bp-NCO)

A three-necked 50 mL round-bottom flask equipped with a magnetic stirring bar, reflux condenser, and nitrogen inlet was covered with aluminium foil and charged with 4-hydroxybenzophenone (3.0 g, 1 eq., 15.13 mmol) and hexamethylene diisocyanate (HMDI, 12.73 g, 5 eq., 75.67 mmol). The reaction mixture was stirred for 16 h at 100 ºC under nitrogen in the dark (SI-Scheme 1). The reaction mixture was cooled to ambient temperature and precipitated in hexane (100 mL). The resulting white precipitate was filtered off and washed with three aliquots of hexane (3 × 40 mL) to remove residues of hexamethylene diisocyanate. The product was dried at 50 ºC under vacuum for 24h (yield = 4.90 g, 88%) and characterized by ^{1}H-NMR (SI-Fig. 1), and FT-IR spectroscopy (SI-Fig. 2).
^{1}H-NMR (300MHz, CDCl3): δ = 7.78-7.84 (m, 5H), 7.59 (t, 1H). 7.48-7.50 (m, 2H), 7.23-7.26 (m, 2H), 3.26-3.38 (m, 4H), 1.43-1.63 (m, 8H).

Derivatization of CNCs with Bp-NCO

The CNCs were functionalized with benzophenone by reaction of surface hydroxyl groups with Bp-NCO. Thus CNCs (0.50 g, 1 equivalent, 3.1 mmol, assuming that three hydroxyl groups are available from *every* cellulose repeat unit and that all molecules are accessible, which is obviously not the case, as the majority is "buried" within the CNCs) were dispersed in anhydrous DMF (200 mL) *via* stirring for 30 min and subsequent sonication for 2 h in a three-necked 250 mL round-bottom flask that was covered with aluminium foil and equipped with a magnetic stirring bar, reflux condenser, and nitrogen inlet. To the CNC dispersion a catalytic amount of DBTDL (1 drop) and Bp-NCO (1.24 g, 1.1 eq., 3.4 mmol) were added and the reaction mixture was stirred for 16 h at 100 ºC under nitrogen in the dark. The product was separated by centrifugation at 8000 rpm for 15 min and the supernatant was discarded and replaced with fresh anhydrous DMF (100 mL). This process was repeated 4 times. After the last washing step, the modified CNCs were kept suspended in DMF in the round bottom flask covered with aluminium foil. The yield of reaction, measured gravimetrically by drying an aliquot of the final dispersion, was 0.53g.

Dispersion of Bp-CNCs and CNCs

An ultrasonication bath from Bandelin Sonorex Technik (RL 70 UH) operating at 40 kHz was used to disperse the CNCs and Bp-CNCs in different solvents at room temperature. A DMF dispersion of Bp-CNC (43 mL of 7 mg/mL, 301 mg) was diluted with DMF (17 mL) to create a dispersion with a Bp-CNC concentration of 5 mg/mL. Freeze-dried CNCs (unmodified) were dispersed in DMF at a concentration of 5 mg/mL. DMF suspensions of Bp-CNCs and CNCs were stirred for 30 min and then sonicated for 3 h.

Solution-Casting of Bp-CNC Films

A DMF dispersion of as-prepared Bp-CNCs was cast into a Teflon® Petri dish and the solvent was evaporated by heating the in an oven at 70 ºC over the course of 24 h. The resulting 40-50 µm thick film was subsequently placed in a vacuum oven at 70 ºC for 48 h to complete the removal of DMF.

Fabrication of EO-EPI/Bp-CNC and EO-EPI/CNC Nanocomposites

A stock solution of EO-EPI was prepared by dissolving EO-EPI in DMF at a concentration of 50 mg/mL by stirring at room temperature for 48 h. Nanocomposites comprising 10 or 20% w/w of Bp-CNC or 10% w/w of the neat CNCs (as reference material) were prepared by combining appropriate amounts of DMF dispersions of Bp-CNC (20 mL and 40 mL DMF dispersion of Bp-CNC for 10% w/w and 20% w/w nanocomposites respectively) or neat CNCs (20 mL DMF dispersion of Bp-CNC for 10% w/w nanocomposite) with the EO-EPI stock solution (18 mL and 16 mL DMF solution for 10% w/w and 20% w/w nanocomposites respectively)to create 1 g of each respective nanocomposite. The mixtures were stirred for 30 min and sonicated for a further 1 h, before they were cast into Teflon® Petri dishes (80 mL capacity). The DMF was evaporated in an oven at 70 ºC over the course of 24 h and the resulting films were subsequently dried in a vacuum oven at 70 ºC for another 48 h. After the complete removal of the solvent (as verified via TGA), the nanocomposite films were reshaped by compression molding in a Carver® press between Teflon® sheets at a temperature of 80 ºC and a pressure of 5000 psi for 3 min, using spacers to yield films having a thickness in the range of 50-80 µm. The EO-EPI/Bp-CNC nanocomposites were kept in the dark.

Photoreaction of Bp-CNCs in DMF Dispersions, Bp-CNC films, and EO-EPI/Bp-CNC Nanocomposites

A 8 W UV lamp from Ultra Violet Products (UVP) operating at 302 nm was used to trigger the photoreaction of Bp-CNCs in DMF dispersions, films made from Bp-CNCs only and nanocomposites of EO-EPI/Bp-CNC. During UV irradiation, a distance of 4 cm was maintained between the UV lamp and quartz cuvettes or Bp-CNCs/nanocomposite films mounted onto quartz slides.

Atomic Force Microscopy (AFM) and Optical Microscopy

To investigate the surface morphology of as-prepared and UV-exposed nanocomposite films, atomic force microscopy (AFM) and optical microscopy studies were performed. Briefly, a photomask was applied onto a 70 µm thick 10% w/w EO-EPI/Bp-CNC nanocomposite film in order to selectively crosslinked the UV exposed portion. After 120 min of UV exposure at 302 nm, the film was mounted onto a glass

microscopy slide to analyze the surface morphology at the interface between the UV exposed and unexposed portions. An AFM Nano Wizard II (JPK Instruments) microscope was used at ambient temperature to acquire the AFM images. The scans were performed in tapping mode in air using silicon cantilever (NANO WORLD, TESPA-50) with spring constant of 42 N/m at the resonance frequency of 320 kHz with a scan rate of 1 line/second. Optical microscopy images were taken on an Olympus BX51 microscope equipped with a DP72 digital camera.

Dynamic Mechanical Analysis (DMA)

To determine the mechanical properties of the nanocomposites, DMA measurements were carried out using a TA instruments model Q800 dynamic mechanical analyzer. All tests in the dry state were carried out in tensile mode using a temperature sweep method from -70 ºC to 100 ºC with a frequency of 1 Hz, a strain amplitude of 15 µm, a gap distance between jaws of ~10 mm and a heating rate of 3 ºC/min. Samples for these experiments were of rectangular shape with a width of ~6 mm and a length of ~15 mm. To determine the mechanical properties of the nanocomposites in the water-swollen state, DMA experiments were conducted in tensile mode with a submersion clamp with temperature sweep in the range of 30-50 ºC, a heating rate of 1 ºC/min, a constant frequency 1 Hz, strain amplitude of 15 µm and a fixed gap distance between jaws of 15 mm. The samples used for these experiments were of rectangular shape with a width of ~6 mm and a length of ~20 mm. For the submersion measurements, samples were swelled in deionized water for 48 h at room temperature, and all measurements were carried out while the samples were immersed in deionized water.

Shape Memory and Light-Activated Shape Fixing Measurements

In order to demonstrate shape memory and light activated shape fixing capabilities of nanocomposites, films of the 10% w/w EO-EPI/Bp-CNC nanocomposite were swollen in the deionized water for 2 days under the dark conditions, twisted into a coiled form around a glass rod to program a temporary shape and dried at room temperature for 24 h. After drying, half of the coil was masked with aluminium foil, while the other half was irradiated with UV light (302 nm, 8 W, 120 min, RT). The sample was subsequently immersed in water at room temperature and the resulting movement was recorded with a digital camera at different time intervals (0-30 min).

Results and Discussion

The CNCs used in this study were isolated from tunicates (*Styela clava*) collected from floating docks in Point View Marina (Narragansett, RI) *via* sulfuric acid hydrolysis using the standard protocols as reported previously.[21, 27, 36] TEM images of DMF dispersions of isolated CNCs reveal that the nanocrystals are well individualized and they exhibit the characteristic rod-shaped morphology (Fig. 2a). Dimensions of isolated CNCs were determined from TEM images, resulting an average length of 1800 ± 600 nm, a width of 25 ± 5 nm, and an aspect ratio (length/width) of 72.

The CNCs were functionalized by reacting a portion of the surface hydroxyl groups with an excess of 4-benzoylphenyl (6-isocyanatohexyl) carbamate (Bp-NCO) at elevated temperature, using a catalytic amount of dibutyltindilaurate (DBTDL) (Scheme 1a).

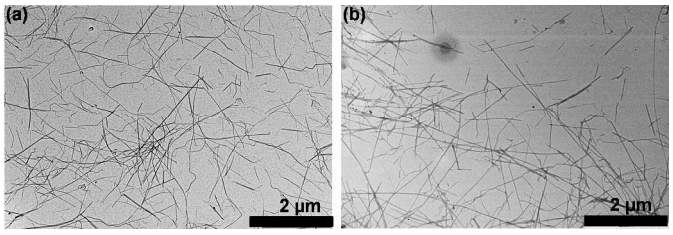

Fig. 2 Transmission electron microscopy (TEM) images of (a) H_2SO_4 hydrolyzed CNCs from tunicates and (b) benzophenone derivatized CNCs (Bp-CNCs). Samples were prepared from 0.1 mg/mL DMF dispersions by drop casting on carbon-coated copper grids.

After separating the resulting Bp-CNCs from the reaction mixture by way of centrifugation, they were stored in DMF and handled in the dark, before being characterized by TEM, FT-IR and UV-Vis techniques. TEM images of Bp-CNCs show that they remained well-individualized after deposition from the DMF dispersion and that they maintained the same characteristic rod-shape morphology as unmodified CNCs (Fig. 2b). The average length (1850 ± 550 nm), width (26 ± 5 nm), and aspect ratio (71) of the Bp-CNCs, determined again from TEM images, were found to be statistically identical to those of the unmodified CNCs. The FT-IR spectrum of Bp-CNCs (SI-Fig. 2) shows a characteristic carbonyl stretching at 1702 cm^{-1}, which corresponds to the urethane linkage formed upon attachment of the Bp moiety and is not observed in the spectrum of the neat CNCs. Furthermore, the absence of a peak at 2265 cm-1, corresponding to the isocyanate groups, confirms that the unreacted Bp-NCO was completely removed during purification. The extent of surface functionalization of Bp-CNCs (SI-Fig. 3), was determined by UV-Vis spectroscopy to be 157 mmol/kg, using a calibration curve of solutions of Bp-NCO (SI-Fig. 4) and comparing the absorbance maximum of the benzophenone motif at 290 nm.

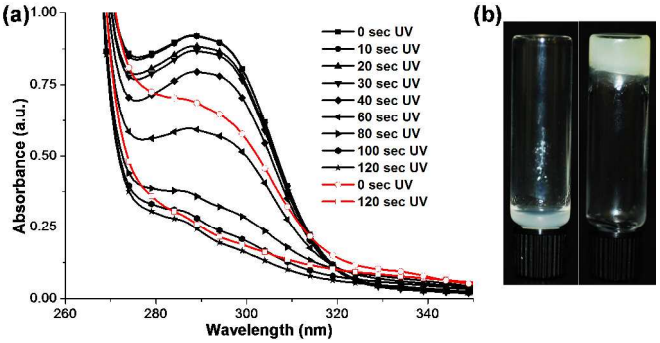

Fig. 3 (a) UV-Vis absorption spectra of a solution of Bp-NCO (black symbols, 10 µg/mL) and a dispersion of Bp-CNC (red symbols, 125 µg/mL) in DMF as function of UV irradiation time (302 nm, 8 W, room temperature), as indicated in the graph. (b) Pictures showing a DMF dispersion (5 mg/mL) of Bp-CNC before (left, liquid) and after (right, gel) exposure to UV light (302 nm, 8 W, 30 min, room temperature).

To demonstrate the light-induced reaction of the benzophenone motifs in the functionalized nanomaterials, a dilute DMF dispersion of Bp-CNCs (125 µg/mL) and a dilute DMF solution of Bp-NCO (10 µg/mL) were exposed to the light of a low-power UV lamp operated at 302 nm. UV-visible spectra (Fig. 3a) show that the characteristic absorbance of the Bp group at 290 nm rapidly decreased in both cases with increasing in irradiation time, to vanish within a period of 120 sec. This effect mirrors previously reported experiments,[48, 49] and is consistent with a sequence that starts with the promotion of one electron from the nonbonding *n* orbital to an antibonding π^* orbital of the carbonyl group of the benzophenone motif upon light-absorption, this n-π^* transition yields a biradicaloid triplet state where the electron-deficient oxygen n-orbital is electrophilic. On the basis of a vast body of literature on the mechanism of the photoreaction of benzophenones,[48, 49] it is assumed that the biradical can readily abstract a hydrogen radical from a neighboring molecule and that a new carbon-carbon bond is formed between the two radicals emerging from this process (Scheme 1b). Interestingly, but not unexpectedly, a more concentrated DMF dispersion of Bp-CNCs (5 mg/mL) turned into gel upon irradiation with UV light (Fig. 3b); while in this case a longer exposure time (30 min) was necessary, this example further supports the formation of covalent bonds between Bp-CNCs and the eventual development of a Bp-CNC network, which is the basis of the observed gelation.

After confirming the UV-triggered reaction of Bp-CNCs in solution and dispersion, we sought to demonstrate cross-linking in solid samples consisting of Bp-CNC only, *i.e.*, without EO-EPI as a polymeric host. Hence, Bp-CNC films with a thickness of 50 µm were cast from the DMF dispersion, small rectangular pieces were cut, and a portion of these samples were subjected to UV irradiation; in this case each side of the sample was exposed to the light of a low-power UV lamp operated for 60 min to facilitate complete reaction. To test dispersibility the samples thus treated and un-irradiated reference samples were placed in water for 24 h before ultrasonication (40 kHz) for 30 min. As expected, the as-prepared Bp-CNC films disintegrated during sonication, while the UV-treated film remained intact, suggesting that also in this case a robust, covalently crosslinked CNC network had been formed (Fig. 4).

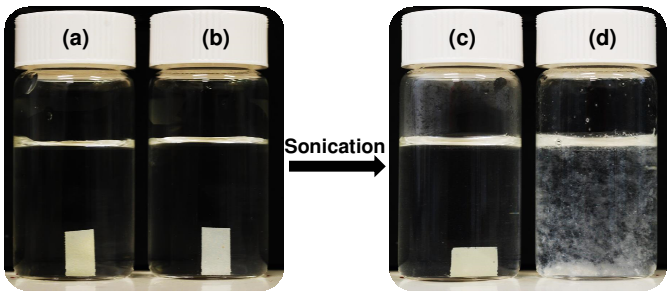

Fig. 4 Pictures of solution-cast 50 µm thick Bp-CNC films after just placing them in deionized water (a, b) and after immersion in water for 24 h followed by 30 min sonication (c, d). Prior to the experiment, the sample shown in (a) and (c) was exposed to UV light (302 nm, 8 W) for 120 min at RT, whereas the sample shown in (b) and (d) was used as prepared.

To investigate if the optically-induced crosslinking influences the mechanical properties of the Bp-CNC films, DMA tests were carried out on neat Bp-CNC films before and after UV exposure. In the dry state, no substantial difference can be discerned (SI-Fig. 5); at 25 °C both materials display a tensile storage modulus E' of ca. 3.9 ± 201 GPa (Table 1). This value is comparable to that of a neat film of unmodified CNCs (4 GPa),[47] which is not surprising as the mechanical properties of neat CNC films are strongly influenced by their porosity and the aspect ratio of the CNCs.[50] Furthermore, we note that the degree of functionalization of the present Bp-CNCs is quite low (157 mmol/kg) so that many OH groups remain on the CNC surface and contribute to the interactions among the particles.[35, 37] Upon placing the samples in water to reach equilibrium swelling (but without applying ultrasounds) E' was reduced in both cases. While in the case of the untreated samples E' decreased to 765 ± 56 MPa, the reduction was less pronounced in the case of the UV-treated material, which displayed an E' of 1299 ± 42 MPa. This situation is consistent with the interpretation that in the water-swollen state non-covalent hydrogen-bonding interactions between the Bp-CNCs are reduced due to competitive hydrogen bonding with water, whereas the covalent cross-links among the Bp-CNCs, which are only present in the UV-irradiated films, remain essentially unaffected and continue to support stress-transfer in the CNC network. The swelling behaviour of the here-reported neat Bp-CNCs films in water before and after UV irradiation was also investigated. Expectedly, untreated Bp-CNC films showed a much greater water up-take (~93% w/w swelling) than the UV-treated Bp-CNC films (~63% w/w swelling) after 48 h at room temperature (SI-Table 1).

Lastly, nanocomposites comprising a rubbery ethylene oxide/epichlorohydrin copolymer (EO-EPI) matrix and 10 or 20% w/w Bp-CNCs were prepared *via* solution casting (SI-Fig. 6a) using DMF as a common solvent. After drying, the nanocomposites thus made were compression molded at a temperature of 80 ºC and a pressure of 5000 psi to yield 50-80 µm thick transparent films with a homogeneous appearance (SI-Fig. 6b). We recently reported that the possibility to moderate

CNC-CNC interactions in a matrix polymer upon exposure to water can also be used in the context of shape-memory materials.[29] Fixing of a temporary shape was accomplished in nanocomposites based on a rubbery polyurethane matrix and unmodified CNCs upon stretching the materials in a water-swollen state, *i.e.* under conditions in which the CNCs are largely "decoupled", from their original shape to a maximum strain of several hundred % and drying the film under fixed stress. The stress was subsequently released, and the samples retained an elongated shape on account of stabilization through an elongated CNC network that had formed upon drying. When these samples were immersed in water, the CNC network disassembled and the rubber elasticity of the matrix served as driving force to promote relaxation to the original shape.

Table 1 Summary of mechanical properties of Bp-CNC films and nanocomposites.

Samples	As-prepared samples		After UV irradiation[a]		After aqueous swelling[b]	
	at - 60 °C E'(MPa)	at 25 °C E'(MPa)	at - 60 °C E'(MPa)	at 25 °C E'(MPa)	Before UV at 35 °C E'(MPa)	After UV[a] at 35 °C E'(MPa)
EO-EPI	3372 ± 290	4.3 ± 0.2	3212 ± 240	4.1 ± 0.50	NA	NA
EO-EPI/Bp-CNC 10% w/w	5644 ± 532	222 ± 4	7373 ± 380	293 ± 26	21 ±3	66 ± 6
EO-EPI/Bp-CNC 20% w/w	5172 ± 534	407 ± 26	6446 ± 460	508 ± 50	75 ± 12	124 ±5
EO-EPI/CNC 10% w/w	6194 ± 189	331 ± 2	6185 ± 396	328 ± 16	NA	NA
Bp-CNC	NA	3902 ± 201	NA	3775 ± 167	765 ± 56	1299 ± 42
Neat CNC	NA[c]	4000[c]	NA[c]	NA[c]	NA[c]	NA[c]

[a]DMA experiments were performed after 120 min of UV exposure (302 nm, 8 W, RT) to the samples at room temperature. [b]DMA experiments were performed in submersion mode with water, after equilibrium swelling for 48 h in water at room temperature. [c]Data taken from reference 43. Experimental data points quoted represent averages of N = 3-5 experiments ± s.d. NA = not available.

We explored here in a qualitative manner if this working principle could be combined with the above-reported light-stimulated mechanically adaptive behaviour of Bp-CNCs, noting, however, that EO-EPI is not an ideal matrix for this purpose, due to its poor elastic recovery. Thus, a helically-shaped coil was prepared from a strip of the nanocomposite consisting of EO-EPI and 10% w/w CNC-Bp by wetting the as-prepared sample, forming it into the desired shape, before drying it to fix the temporary helical shape through the formation of a hydrogen-bonded CNC network (Fig. 5). Half of the coiled sample was subsequently masked, whereas the other half was exposed to UV light. The sample was subsequently immersed in deionized water at 25 ºC and movement of coil was recorded with a digital camera as function of immersion time (SI-Fig. 7). Fig. 5 shows clearly that after immersion for 30 min, the unexposed portion of the sample had recovered to the original shape (*i.e.* a rectangular strip), whereas the part exposed to UV light retained the coiled form. Thus, the exposed portion of the sample has been locked in the coiled shape, by covalent crosslinking of the Bp-CNCs between each other and with the matrix.

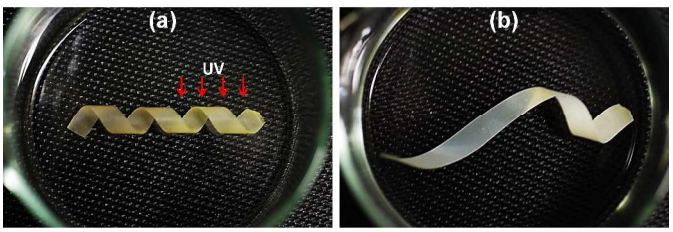

Fig. 5 Pictures of 10% w/w EO-EPI/Bp-CNC film, demonstrating shape memory and light activated shape fixing capabilities of the nanocomposites. Right half portion of coil (a) was exposed to UV light (302 nm, 8 W, 120 min, RT) and left half portion was masked with aluminium foil during UV exposure. (b) Sample after immersion in water at room temperature.

To demonstrate that the UV light induced crosslinking could be used to photopattern the nanocomposites and create mechanically graded structures, two rectangular strips of the 10% w/w EO-EPI/Bp-CNC (3.5 × 0.8 cm) nanocomposites were prepared. In one case, the central (1.5 cm) portion of the strip was masked with aluminium foil and both the edges were exposed to UV light at 302 nm for 120 min. This process was applied with the intent to stiffen both edges of the strip while leaving the masked central portion unchanged. When a compressive force was applied, both the edges remained straight, whereas the central portion (*i.e.* the soft part) bent uniformly (Fig. 6). When the same force was applied to an untreated reference film, the sample displayed a more uniform deformation (Fig. 6)

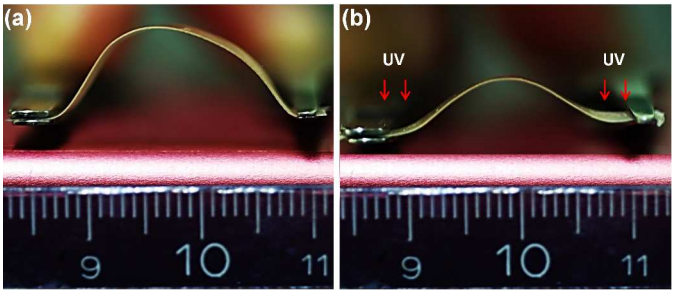

Fig. 6 Pictures of films of EO-EPI/Bp-CNC 10% w/w nanocomposite having lengths of 3.5 cm, showing mechanically gradient behavior. Film (a) is unexposed to the UV, while in case of (b) both edges (1.0 cm) exposed to the UV

irradiation at 302 nm (8 W, 120 min, RT) and center 1.5 cm portion was masked with aluminium foil during UV irradiation.

Atomic force microscopy (AFM) and optical microscopy were used to study the surface topology of nanocomposite films before and after exposure to UV light. In case of AFM measurements, tapping mode in air was used to analyze the surface morphology of 10% w/w EO-EPI/Bp-CNC nanocomposite film at room temperature. Figs. 7a and b show AFM phase contrast images and SI-Fig. 8b shows AFM amplitude image reveal a clear topology difference at the interface between the exposed and non-exposed portions. The AFM topography revealed distinct difference between the stiff and soft segments in the photopatterned film. In parallel with other obtained results, this is likely due to the crosslinking effect of Bp-CNCs in the UV exposed nanocomposite resulting in hard segments, while as-prepared nanocomposite comparatively preserved soft segments (Fig. 7). The same trend was also observed by Tria *et al.* while preparing polymer brushes *via* photopatterning using benzophenone chemistry.[42] Optical microscopic images (Fig. 7c) in normal light and (Fig. 7d) under UV light also displays the corresponding interface difference between UV exposed and unexposed part, respectively.

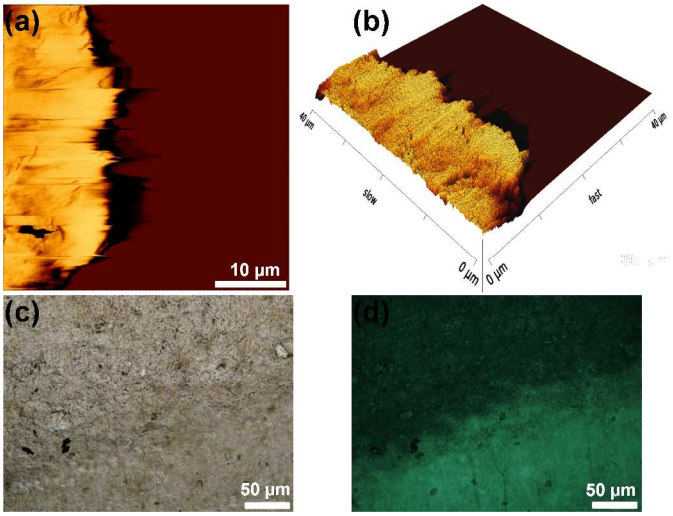

Fig. 7 (a, b) Atomic force microscopy (AFM) and (c, d) optical microscopy images of 10% w/w EO-EPI/Bp-CNC nanocomposite. AFM Phase image (a) and corresponding 3D image (b) show difference in morphology at the interface between the stiff state as a result of UV exposure at 302 nm for 120 min and soft state which is unexposed to the UV. Optical microscopic image (c) in normal light and (d) under UV light also displays the corresponding interface difference between UV exposed and unexposed part, respectively.

To demonstrate the light-responsive mechanically adaptive behavior of these polymer nanocomposites, DMA experiments were performed as a function of temperature, before and after UV irradiation and comparisons were made with films of the neat polymer matrix and of nanocomposites of EO-EPI with unmodified CNCs (Table 1). The neat EO-EPI matrix displays tensile storage modulus (E') of 3.3 GPa in the glassy state at -60 °C (SI-Fig. 9), and of 4.3 MPa in the rubbery state at 25 °C. As can be expected, the DMA traces of neat EO-EPI and UV-treated EO-EPI are virtually identical (SI-Fig. 9). The as-cast nanocomposites comprising 10% or 20% w/w Bp-CNC showed an increased stiffness at -60 °C, where E' rose from 3.3 GPa (neat EO-EPI) to over 5 GPa in case of both nanocomposites. The reinforcement was much more profound in the rubbery regime at 25 °C where E' increased from 4.3 ± 0.2 MPa for the neat EO-EPI to 222 ± 4 MPa for the nanocomposite with 10% w/w Bp-CNCs, and to 407 ± 26 MPa for the nanocomposite with 20% w/w Bp-CNCs. The pronounced reinforcement above the glass transition temperature (T_g ~ -30 °C) is in agreement with previous results, which revealed that the mechanical properties in the rubbery regime are, at the concentrations studied, dominated by the formation of a CNC network.[32] When the Bp-CNC/EO-EPI nanocomposite films were irradiated with UV light, a dose-dependent increase of the nanocomposites' stiffness was observed (SI-Fig. 10). When exposed to the light of an 8 W UV lamp operated at 302 nm E' of a nanocomposite with 10% w/w Bp-CNCs increased with exposure time from an average value of 222 ± 4 MPa to reach an average value of 293 ± 26 MPa after 120 min and no further increase in E' was observed, indicating completion of the crosslinking reaction. A similar trend was observed for the nanocomposites with 20% w/w Bp-CNCs, where E' at 25 °C increased from 407 ± 26 MPa to 508 ± 50 MPa (Fig. 8a). DMA traces of both UV exposed nanocomposites also displayed an increase in E' from ca. 5.3 GPa to ca. 7 GPa at –60 °C, *i.e.*, below T_g. In order to confirm that the observed mechanical changes are indeed due to light-induced formation of covalent bonds between the CNCs and the CNCs and the matrix polymer (Fig. 8a). Set of control experiments was also performed in which nanocomposites comprised of EO-EPI and 10% w/w of unfunctionalized CNCs were subjected to mechanical testing before and after UV exposure under identical conditions (SI-Fig. 11). As expected, these experiments demonstrate that E' of these nanocomposites remains virtually unaffected by the UV irradiation.

Based on the notion that only a comparably small fraction of the hydroxyl groups on the CNC surface are decorated with Bp groups, exposure to water should therefore also affect the interactions among the Bp-CNCs and between Bp-CNCs and the matrix. Fig. 8b shows the DMA plots of EO-EPI/Bp-CNC nanocomposites in the submersion state, after immersing them in water until equilibrium swelling had been reached. The DMA traces of both sets of EO-EPI/Bp-CNC nanocomposites showed significant improvement of E' for UV treated films compared to as-prepared films. This is presumably due to competitive hydrogen bonding with water in the swollen state in which all non-covalent hydrogen-bonding interactions between the Bp-CNCs are turned off in UV unexposed samples, whereas the covalent cross-links among the Bp-CNCs and Bp-CNC-polymer matrix, which are only present in the UV-irradiated nanocomposites. For instance, E' increased from 21 ± 3 MPa for as-prepared nanocomposite with 10% w/w Bp-CNCs to 66 ± 6 MPa for UV treated nanocomposite (~300% increase).

The nanocomposites with 20% w/w of Bp-CNCs paint the similar picture, where *E′* increased from 75 ± 12 MPa for as-prepared nanocomposite to 124 ± 5 MPa for UV treated nanocomposite. The swelling behaviour of here-reported nanocomposites was also investigated in water before and after the UV exposure. Expectedly, as-prepared EO-EPI/Bp-CNC nanocomposites (10 and/or 20% w/w) exhibited higher degree of swelling (~20% w/w) than the UV treated nanocomposites (~8% w/w) after 48 h at room temperature (SI-Table 1). This illustrates the importance of linking between the matrix and filler when hydrogen bonding is 'turned off'.

The mechanical data of EO-EPI/Bp-CNC nanocomposites in the dry state were further analyzed in the context of the percolation model (SI-Fig. 12), which has been used extensively to explain the mechanical properties of nanocomposites reinforced with anisotropic fillers.[11, 51, 52] The percolation model explains the tensile storage modulus of filler reinforced materials assuming filler-filler interactions are predominate, resulting in interconnected network and facilitates the transfer of stress though the composite. An exponential increase in stiffness is observed above the percolation threshold *i.e.* the level, above which sufficient filler particles are present to form network. As previously discussed, owing to low surface functionalization (*i.e.* 157 mmol/kg of benzophenone functionalization on the CNCs, versus at least 1100 potential functionalization points predicted[35, 37]), substantial amount of hydroxyl groups still remain on the Bp-CNC surface to form the percolating network *via* hydrogen bonding interactions. Therefore, due to the H-bonding interactions of Bp-CNCs in nanocomposites, *E′* values for as-prepared EO-EPI/Bp-CNC nanocomposites matched well with the predicted percolation model published for EO-EPI/CNC nanocomposites[32] (SI-Fig. 9). However, after the UV exposure, Bp-CNCs undergo covalent crosslinking with polymer matrix as well as with other Bp-CNCs, increasing both filler-filler and filler-matrix interactions and resulting in *E′* values shifted slightly above the percolation model predictions.

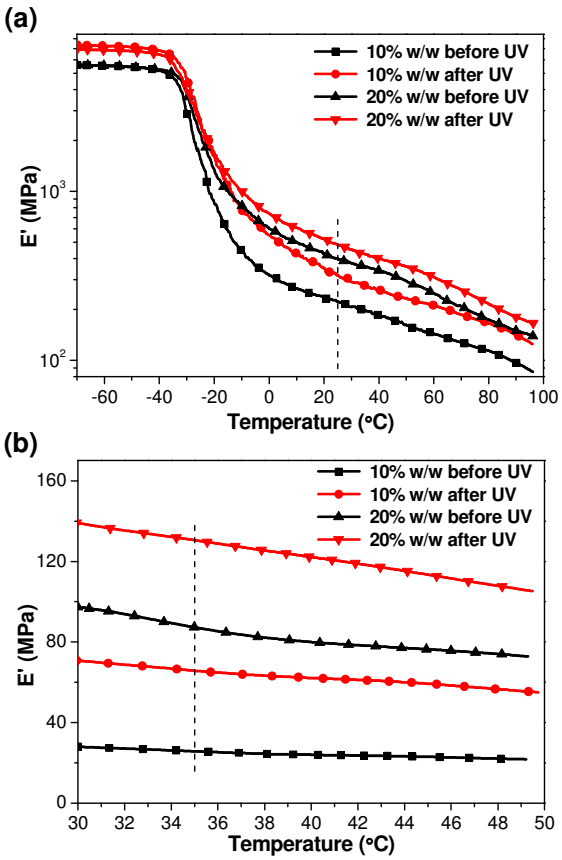

Fig. 8 Dynamic mechanical analysis (DMA) traces of nanocomposites composed of EO-EPI and 10% or 20% w/w Bp-CNC in dry (a) and water-swollen (b) state before (black symbols) and after (red symbols) UV exposure (302 nm, 8 W, 120 min, RT). Shown are plots of the storage modulus *E′* against temperature (note: in (a) Y axis is logarithmic and in (b) it is linear).

Conclusions

In summary, we have shown that CNCs decorated with benzophenone moieties are highly photoreactive and readily form covalent bonds with each other and/or with surrounding macromolecules when incorporated into a polymer matrix. The chemistry used here to modify CNCs is really straightforward and might be readily implemented with commercially used CNCs. Films and coatings consisting of CNCs only have been demonstrated to be useful for practical applications including optically transparent papers and tunable reflective filters and sensors; however, one widely acknowledged problem associated with this family of materials is their highly hygroscopic nature and the fact that properties can change in a dramatic way in humid environments. We have shown here that this problem can be readily mitigated upon exposing Bp-CNCs films to UV light to change the wettability. The new EO-EPI/Bp-CNCs nanocomposites are multi-responsive (light/water) and exhibit the expected mechanical switching characteristics in terms of a pronounced stiffness increase upon exposure to UV light, as well as a reduced swelling and softening upon exposure to water. Finally, we also show in

qualitative manner that before UV exposure these new nanocomposites exhibited shape memory properties and after UV irradiation displayed shape fixing properties. It is worthwhile to note that these materials were not designed for shape memory purpose as EO-EPI is not an ideal matrix for this purpose. But this approach could be easily extended to use Bp-CNCs with more elastic matrix, *e.g.* polyurethane. The photopatterning ability of EO-EPI/Bp-CNC nanocomposites opens up the use of these materials for wide range of potential applications.

Acknowledgements

The authors gratefully acknowledge financial support from the Swiss National Science Foundation (NRP 62: Smart Materials, Nr. 406240_126046) and the Adolphe Merkle Foundation.

Notes

Adolphe Merkle Institute, University of Fribourg, Rte de l'Ancienne Papeterie, CH-1723 Marly 1, Switzerland
Corresponding Author: johan.foster@unifr.ch

Electronic Supplementary Information (ESI) available: Swelling behaviour of nanocomposites, a synthetic scheme for Bp-NCO synthesis, ^{1}H-NMR spectrum of Bp-NCO, FT-IR along with UV-Vis spectra of Bp-NCO and Bp-CNC, schematic representation for the nanocomposites preparation, shape-memory photographs of nanocomposites, DMA data plots not presented in the paper and percolation model predictions for nanocomposites.

References

1. S. Pavlidou and C. D. Papaspyrides, *Prog. Polym. Sci.*, 2008, **33**, 1119-1198.
2. G. Ramorino, F. Bignotti, L. Conzatti and T. Ricco, *Polym. Eng. Sci.*, 2007, **47**, 1650-1657.
3. S. Sinha Ray and M. Okamoto, *Prog. Polym. Sci.*, 2003, **28**, 1539-1641.
4. M. Rahmat and P. Hubert, *Compos. Sci. Technol.*, 2011, **72**, 72-84.
5. G. Pandey and E. T. Thostenson, *Polym. Rev.*, 2012, **52**, 355-416.
6. G. Choudalakis and A. D. Gotsis, *Eur. Polym. J.*, 2009, **45**, 967-984.
7. S. J. Eichhorn, A. Dufresne, M. Aranguren, N. E. Marcovich, J. R. Capadona, S. J. Rowan, C. Weder, W. Thielemans, M. Roman, S. Renneckar, W. Gindl, S. Veigel, J. Keckes, H. Yano, K. Abe, M. Nogi, A. N. Nakagaito, A. Mangalam, J. Simonsen, A. S. Benight, A. Bismarck, L. A. Berglund and T. Peijs, *J. Mater. Sci.*, 2010, **45**, 1-33.
8. K. Shanmuganathan, J. R. Capadona, S. J. Rowan and C. Weder, *Prog. Poly. Sci.*, 2010, **35**, 212-222.
9. D. Klemm, F. Kramer, S. Moritz, T. Lindström, M. Ankerfors, D. Gray and A. Dorris, *Angew. Chem. Int. Ed.*, 2011, **50**, 5438-5466.
10. N. Follain, S. Belbekhouche, J. Bras, G. Siqueira, S. Marais and A. Dufresne, *J. Membrane Sci.*, 2013, **427**, 218-229.
11. Y. Habibi, L. A. Lucia and O. J. Rojas, *Chem. Rev.*, 2010, **110**, 3479-3500.
12. P. Hajji, J. Y. Cavaillé, V. Favier, C. Gauthier and G. Vigier, *Polym. Composite.*, 1996, **17**, 612-619.
13. R. J. Moon, A. Martini, J. Nairn, J. Simonsen and J. Youngblood, *Chem. Soc. Rev.*, 2011, **40**, 3941-3994.
14. M. Pääkkö, M. Ankerfors, H. Kosonen, A. Nykänen, S. Ahola, M. Österberg, J. Ruokolainen, J. Laine, P. T. Larsson, O. Ikkala and T. Lindström, *Biomacromolecules*, 2007, **8**, 1934-1941.
15. S. Camarero Espinosa, T. Kuhnt, E. J. Foster and C. Weder, *Biomacromolecules*, 2013, **14**, 1223-1230.
16. S. Mueller, C. Weder and E. J. Foster, *RSC Adv.*, 2014, **4**, 907-915.
17. M. Jorfi, N. Amiralian, M. V. Biyani and P. K. Annamalai, in *Biomass-based Biocomposites*, ed. V. K. T. a. A. S. Siṅgha, Smithers Rapra Technology Ltd, 2013, pp. 277-304.
18. N. L. Garcia de Rodriguez, W. Thielemans and A. Dufresne, *Cellulose*, 2006, **13**, 261-270.
19. X. Dong, J.-F. Revol and D. Gray, *Cellulose*, 1998, **5**, 19-32.
20. W. Helbert, J. Y. Cavaillé and A. Dufresne, *Polym. Compos.*, 1996, **17**, 604-611.
21. V. Favier, H. Chanzy and J. Y. Cavaille, *Macromolecules*, 1995, **28**, 6365-6367.
22. R. T. Woodhams, G. Thomas and D. K. Rodgers, *Polym. Eng. Sci.*, 1984, **24**, 1166-1171.
23. K. Fleming, D. Gray, S. Prasannan and S. Matthews, *J. Am. Chem. Soc.*, 2000, **122**, 5224-5225.
24. M. Grunert and W. T. Winter, *J. Polym. Environ.*, 2002, **10**, 27-30.
25. S. J. Eichhorn, *ACS Macro Lett.*, 2012, **1**, 1237-1239.
26. R. Sinko, S. Mishra, L. Ruiz, N. Brandis and S. Keten, *ACS Macro Lett.*, 2013, **3**, 64-69.
27. M. Jorfi, M. N. Roberts, E. J. Foster and C. Weder, *ACS Appl. Mater. Interfaces*, 2013, **5**, 1517-1526.
28. S. Kumar, M. Hofmann, B. Steinmann, E. J. Foster and C. Weder, *ACS Applied Materials & Interfaces*, 2012, **4**, 5399-5407.
29. J. Mendez, P. K. Annamalai, S. J. Eichhorn, R. Rusli, S. J. Rowan, E. J. Foster and C. Weder, *Macromolecules*, 2011, **44**, 6827-6835.
30. K. Shanmuganathan, J. R. Capadona, S. J. Rowan and C. Weder, *J. Mater. Chem.*, 2010, **20**, 180-186.
31. K. Shanmuganathan, J. R. Capadona, S. J. Rowan and C. Weder, *ACS Appl. Mater. Interfaces*, 2010, **2**, 165-174.
32. J. R. Capadona, K. Shanmuganathan, D. J. Tyler, S. J. Rowan and C. Weder, *Science*, 2008, **319**, 1370-1374.
33. K. A. Potter, M. Jorfi, K. T. Householder, E. Johan Foster, C. Weder and J. R. Capadona, *Acta Biomater.*, 2014, **10**, 2209–2222.
34. P. K. Annamalai, K. L. Dagnon, S. Monemian, E. J. Foster, S. J. Rowan and C. Weder, *ACS Appl. Mater. Interfaces*, 2013.
35. A. E. Way, L. Hsu, K. Shanmuganathan, C. Weder and S. J. Rowan, *ACS Macro Lett.*, 2012, **1**, 1001-1006.
36. M. V. Biyani, E. J. Foster and C. Weder, *ACS Macro Lett.*, 2013, **2**, 236-240.
37. J. D. Fox, J. R. Capadona, P. D. Marasco and S. J. Rowan, *J. Am. Chem. Soc.*, 2013, **135**, 5167-5174.
38. M. V. Biyani, E. J. Foster and C. Weder, 2014, Submitted.
39. R. E. Galardy, L. C. Craig, J. D. Jamieson and a. M. P. Printz, *J. Biol. Chem.*, 1974, **249**, 3510-3518.
40. G. Dorman and G. D. Prestwich, *Biochemistry*, 1994, **33**, 5661-5673.
41. F. Boscá and M. A. Miranda, *J. Photoch. Photobio. B*, 1998, **43**, 1-26.
42. M. C. Tria, J. Y. Park and R. Advincula, *Chem. Commun.*, 2011, **47**, 2393-2395.

43. S. K. Christensen, M. C. Chiappelli and R. C. Hayward, *Macromolecules*, 2012, **45**, 5237-5246.
44. G. Temel, B. Enginol, M. Aydin, D. K. Balta and N. Arsu, *J. Photoch. Photobio. A*, 2011, **219**, 26-31.
45. K. H. Hong and G. Sun, *Carbohydrate Polymers*, 2008, **71**, 598-605.
46. K. H. Hong, N. Liu and G. Sun, *European Polymer Journal*, 2009, **45**, 2443-2449.
47. J. R. Capadona, O. Van Den Berg, L. A. Capadona, M. Schroeter, S. J. Rowan, D. J. Tyler and C. Weder, *Nat Nanotechnol*, 2007, **2**, 765-769.
48. A. M. Lehaf, M. D. Moussallem and J. B. Schlenoff, *Langmuir*, 2011, **27**, 4756-4763.
49. V. P. Dhende, S. Samanta, D. M. Jones, I. R. Hardin and J. Locklin, *ACS Appl. Mater. Interfaces*, 2011, **3**, 2830-2837.
50. J. Bras, D. Viet, C. Bruzzese and A. Dufresne, *Carbohyd. Polym.*, 2011, **84**, 211-215.
51. S. J. Eichhorn, *Soft Matter*, 2011, **7**, 303-315.
52. V. Favier, G. R. Canova, J. Y. Cavaillé, H. Chanzy, A. Dufresne and C. Gauthier, *Polym. Adv. Tech.*, 1995, **6**, 351-355.

